Mechanical and Crash Performance of Unidirectional Oil Palm Empty Fruit Bunch Fibre-reinforced Polypropylene Composite

Cik Suhana Hassan,[a,]* Veyvein Durai,[a] Mohd Sapuan Salit,[b] Nuraini Abdul Aziz,[b] and Mohd Zuhri Mohamed Yusoff [b]

The mechanical properties of unidirectional oil palm empty fruit bunch (OPEFB) fibre / polypropylene (PP) composites were analysed. The composites were fabricated with unidirectional fibre orientations of 0°, 45°, and 90°, with mass fractions of 25%, 35%, and 45% for each fibre orientation angle. The composites were then subjected to tensile, flexural, and impact testing. Superior tensile, flexural, and impact strengths were observed for the unidirectional composites with 0° fibre orientation angle. A fibre loading of 35% provided the highest tensile strength, while fibre loadings of 25% and 45% yielded the greatest flexural and impact resistances, respectively. The crash performance of the unidirectional composite subjected to low-velocity impact in the automotive bumper fascia was investigated. The composite exhibited significantly improved energy absorption capability and comparable specific energy absorption when compared with the current material being used for the bumper fascia.

Keywords: Biocomposites; OPEFB Fibre; Crashworthiness; Directional orientation

Contact information: a: Mechanical Engineering Department, UCSI University, 1, Jalan Menara Gading, 56000 Cheras, Kuala Lumpur, Malaysia; b: Department of Mechanical and Manufacturing Engineering, University Putra Malaysia, Malaysia;
** Corresponding author: suhana@ucsiuniversity.edu.my*

INTRODUCTION

The applications of fibre-reinforced thermoplastic have evolved rapidly in various areas. Due to its lightweight advantage, the material has been widely employed as front and rear bumpers, in instrument panels, and side mouldings in the automotive industry. The material is also in high demand for its manufacturability. Plastic can be moulded into various designs and shapes to suit market demands, as opposed to metal, which has many constraints.

The current elevated price of plastic has fuelled the search for alternative materials that can reduce costs but still retain the beneficial properties of plastic. The most commonly utilized reinforcement material is glass fibre. However, glass fibre has shown significant disadvantages in terms of cost, density, renewability, recyclability, abrasiveness, and lack of biodegradability. Thus, the use of natural fibre to reinforce plastic is preferable. In addition to enhancing degradability and recyclability, the use of natural fibre offers significant cost and weight reduction. Furthermore, as compared with glass fibre, natural fibres have better sound absorbing efficiency, are more shatter resistant, and have better energy management characteristics. Hence, in automotive parts, biocomposites not only decrease the mass of the components but also reduce the energy needed for production by 80% (Malkapuram *et al*. 2008).

The type of fibre reinforcement in composite materials can be classified as either continuous or discontinuous. Discontinuous fibre composites are normally random in alignment, while continuous fibre composites generally have a preferred orientation. The random alignment of the discontinuous fibres dramatically reduces their strength and modulus (Tanwer 2014). One method of reinforcing as a continuous fibre is by unidirectional fibre alignment. In applications where stiffness and strength are required, the unidirectional reinforcement of the natural fibre is preferable. Many studies have been performed utilizing a unidirectional natural fibre to reinforce a polymer to generate a stiffer yet lightweight material.

Lee *et al*. (2010) evaluated the effect of kenaf fibre orientation on the properties of laminated kenaf fibre-reinforced polypropylene composite. The laminated composite was fabricated using a hot press with four different orientations (random, 0°, 45°, and 90°). The results showed that the composite with the 0° fibre orientation yielded the highest modulus of elasticity and tensile strength compared to the composites with random, 45°, and 90° fibre orientations. Aldousiri *et al*. (2013) fabricated a composite composed of date palm fibre and recycled high-density polyethylene (HDPE). The composite samples, pure HDPE and HDPE with 6% date palm fibre, were prepared *via* hot pressing. The date palm fibres were aligned with 0°. The incorporation of date palm fibre into the recycled HDPE with 0° fibre alignment increased tensile strength from 28 MPa to 38 MPa. Minimal fibre pull-out was observed with a scanning electron microscope (SEM), indicating that the fibre, when oriented parallel with the load applied, effectively preserved the ductility of the HDPE.

Sapiai *et al*. (2014) fabricated a unidirectional kenaf fibre-reinforced epoxy composite. The longitudinal and transverse properties of the composites were tested through tensile and compression tests. The tensile strength of the composite was 42.38 MPa in the longitudinal direction and 3.52 MPa in the transverse direction, and the tensile modulus was 2.43 GPa and 0.33 GPa in the longitudinal and transverse directions, respectively. Biswas *et al*. (2015) studied the physical, mechanical, and thermal properties of jute and bamboo fibre-reinforced unidirectional epoxy composites. The composites were fabricated *via* hot pressing, and the specimens were subjected to flexural testing. The flexural strengths of the jute and bamboo composites were approximately 158 MPa and 226 MPa, respectively, when the loading applied was parallel with the fibre direction. When transverse load was applied to the composites, the strengths of the jute and bamboo composites were 25.7 MPa and 11.89 MPa, respectively. These results show that superior composite properties can be obtained in the longitudinal direction, as compared with the transverse direction and random orientation.

There is growing interest in the exploitation of oil palm fibre as load-bearing constituents in composite material, with the abundant availability of oil palm fibre in Malaysia. As one of the largest palm oil producers, Malaysia generates a large amount of oil palm biomass. Abdullah and Sulaiman (2013) reported an abundance of raw materials available from the palm tree, consisting of approximately 90% of biomass wastes. Oil palm biomass can be derived from three parts of the oil palm tree: oil palm frond, fruit bunch, and oil palm trunk. Fibres from oil palm frond and oil palm trunk are cultivated directly from the plantation site, while the fibres from fresh fruit bunches are obtained from the palm mill site. The process of extracting crude palm oil from the fresh fruit bunches generates a large amount of biomass residue. Among the biomass generated is oil palm empty fruit bunch (OPEFB) fibre, which is extracted by retting from the empty fruit bunch, the fibrous mass remaining after separating the fruits from the fresh fruit bunches. This OPEFB fibre is known to have low density, moderate tensile strength, and a low modulus of elasticity.

While studies on OPEFB fibre composites appear to be growing, its utilization as unidirectional reinforcement material has receiving very limited attention. The focus has primarily been on random oriented OPEFB fibre reinforced polymer composites. This study investigated the effects of fibre orientation on the tensile, flexural, and impact strengths of an OPEFB fibre-reinforced polypropylene (PP) composite. A unidirectional composite with 0° fibre alignment is expected to be stronger and stiffer than the composites with the other fibre alignment angles. As fibre orientation changes from 0° to 90°, the properties of the fibres decline, and the properties of the matrix dominate (Hegde *et al*. 2015), with the load being carried by the much weaker polymeric matrix (Campbell 2003).

This biocomposite could be used to substitute the use of PP in automotive applications, such as for car bumpers. During frontal impact, the front bumper system, which may to some extent protect the car body and passengers, is the first part that receives the collision impact (Davoodi *et al*. 2012). The frontal bumper system consists of three main components: the fascia, the absorber, and the bumper beam (Sapuan *et al*. 2005). The fascia is usually used for aesthetics and for decreasing aerodynamic drag. It cannot tolerate impact energy; thus, it is considered a non-structural component (Davoodi *et al*. 2008). It is hoped that the incorporation of OPEFB fibre in the bumper fascia material will increase its energy absorption capability, allowing it to play a significant role in the event of a collision. To investigate the applicability of this biocomposite material for car bumper fascias, the crash performance of the composite when subjected to low-velocity impact was analyzed using finite element analysis.

EXPERIMENTAL

Composite Fabrication and Testing

The OPEFB fibres obtained from a palm mill site in Selangor, Malaysia, were first soaked in distilled water for 24 h to remove impurities and left to dry. The fibres were then soaked in a 5% sodium hydroxide solution for 2 h, rinsed with distilled water, and allowed to dry for another 24 h at room temperature. The dried fibres were then straightened using a comb and by applying pressure at both ends of the fibres while placing them in a straight position.

Prior to composite fabrication, PP initially in pellet form, obtained from Chemmart Asia Sdn. Bhd., Selangor, Malaysia, was first fabricated as PP sheet. The pellets were oven-dried at 40 °C for 24 h prior to sheet fabrication to remove any moisture content as well as to help eliminate bubbles during fabrication of the PP sheets. The dried PP pellets were weighed precisely to 21.5 g using a measuring balance. The pellets were then placed into a steel mould cavity of 150 mm × 150 mm × 1 mm in size. The PP pellets were evenly spread throughout the mould cavity to provide uniformity during compression moulding. Before placing the pellets, both the top and lower covers were sprayed with a releasing agent to reduce adhesion and help in the removal of the PP sheets after compression moulding. Compression moulding was performed with a temperature of 190 °C for the heating process. Once the compression machine reached the optimum temperature required, the mould was gently placed onto the upper deck of the Technopress-40HC-B hydraulic compression moulding machine (Technovation, Selangor, Malaysia), where the heating occurred. The fabrication process included 7 min of preheating, two instances of venting, and 2 min of hot pressing at 2500 kPa pressure. The mould was then shifted from the upper deck to the lower deck, where cooling and curing occurred for 7 min. Upon completion of the cooling process, the mould was removed from the machine, and the fabricated sheet was gently removed from the mould. The overall process took approximately 16 min to fabricate one PP sheet.

For composite fabrication, the OPEFB fibres were aligned manually in between two PP sheets in a 150 mm × 150 mm × 3 mm mould. A schematic of the sandwiched arrangement is shown in Fig. 1. One piece of the composite was fabricated using two layers of OPEFB fibres sandwiched with three layers of PP sheets. The sandwiched assembly was then subjected to compression moulding at a temperature of 190 °C and a pressure of 2500 kPa. The process included 7 min of preheating, two instances of venting, and 2 min of hot pressing, followed by cooling for 7 min. The composites were prepared with fibre weight ratios of 0%, 25%, 35%, and 45%.

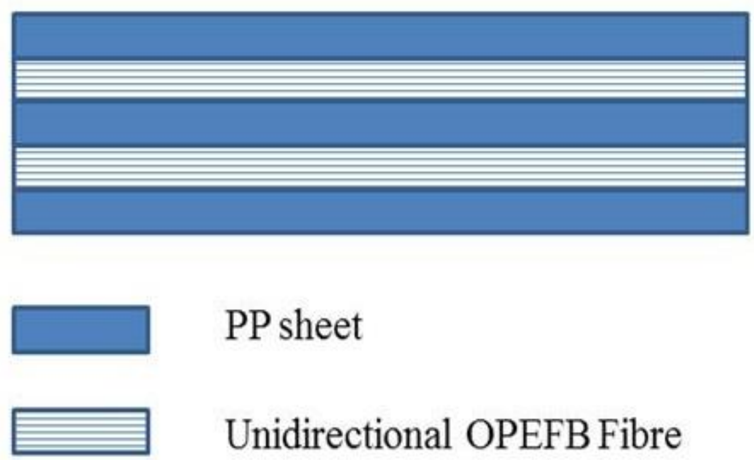

Fig. 1. Schematic of the OPEFB fibre/PP arrangement prior to compression moulding

The composites were then cut for tensile, flexural, and impact testing. The obtained tensile specimens were tested, using an INSTRON 3366 10 kN universal testing machine (INSTRON, Norwood, MA, USA) at a crosshead of 5 mm/min, and the fractured surfaces were investigated *via* scanning electron microscopy (SEM). The flexural tests were conducted using an INSTRON 3365 5 kN universal testing machine (INSTRON, Norwood, MA, USA) at a crosshead of 2 mm/min, and the data was recorded. Charpy impact tests were conducted using a pendulum impact tester, and the energy absorbed per unit width of specimen was investigated.

Finite Element Analysis

A finite element model was used to simulate the impact on the bumper fascia. The simulation was conducted using LS-Prepost and LS-DYNA solver (LSTC, 971, Livermore Software Technology Corporation, Livermore, USA). The selected scenario was the collision of a bumper fascia with a rigid wall. The scenario served as a simple and ideal model to reveal the general characteristics of the impact behavior. A schematic of the finite element setup for the bumper fascia crash analysis is shown in Fig. 2. Full frontal impact against a rigid wall barrier was modelled with an impact speed of 4 km/h. A point mass of

1200 kg was assigned fixed to the bumper fascia. The rigid wall was modelled with equivalent mass.

The fascia was idealised using 6485 shell elements. The composite bumper fascia was modeled with the LS-DYNA material model MAT 55. All contact surfaces were defined using the *AUTOMATIC_SURFACE_SURFACE contact card. No constraints were applied to the bumper, for the restraint was maintained by the global inertia of the vehicle.

For comparison, a baseline model was simulated using the current material employed for bumper structure, which was PP for bumper fascias. The material properties of the baseline model are listed in Table 1. The PP was modelled using material type 24 (MAT_PIECEWISE_LINEAR_PLASTICITY), which requires the stress and strain curve for the material to be defined. The stress-strain graph for the PP is shown in Fig. 3.

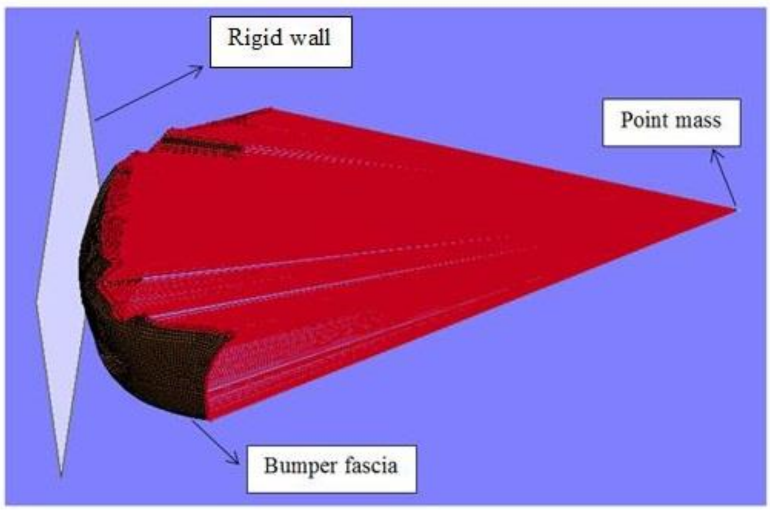

Fig. 2. Finite element analysis model of the bumper fascia impact system

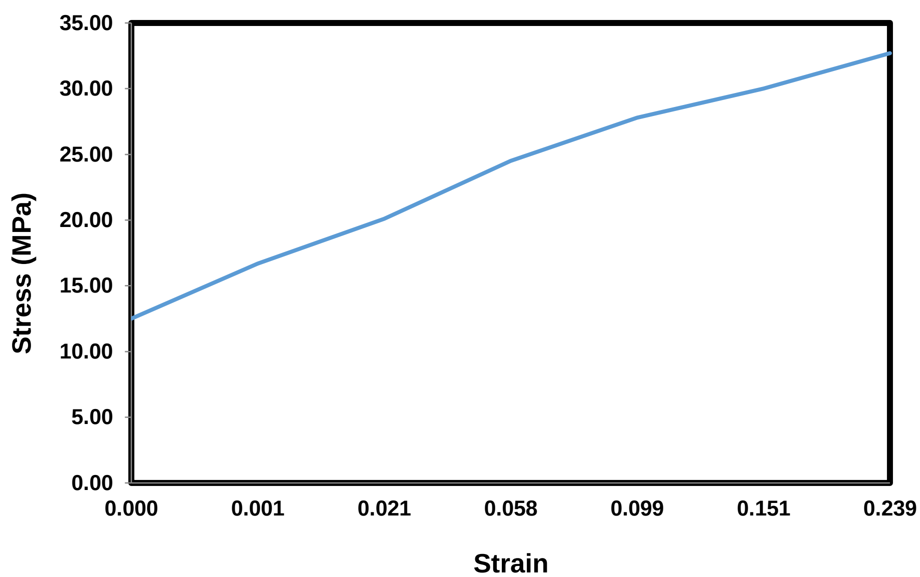

Fig. 3. Stress-strain relation for the baseline model material

Table 1. Material Properties of the Baseline Model

Material	Young's Modulus, *E* (MPa)	Poisson Ratio, *v*	Yield Stress (MPa)	Density, *ρ* (kg/m^3)
PP	632	0.38	12.5	907

RESULTS AND DISCUSSION

Mechanical Performance of the Unidirectional OPEFB Fibre/PP Composite

The composites were made with three different fibre orientation angles and three different fibre weight ratios. Figure 4 shows the tensile stress-strain curve of 25 wt% OPEFB fibre/PP composite.

As shown, all fibre orientations exhibited an initial elastic deformation followed by nonlinear deformation and failure. Similar trends were observed for composites made of 35 wt% fibre, as shown in Fig. 5. Figure 6 shows the typical stress-strain response for 45 wt% OPEFB fibre/PP composite. The initial stress-strain response leading up to the peak stress was relatively similar to the 25 wt% and 35 wt% fibre composites. However, in contrast, the post-peak stress response was very ductile, particularly for composites with fibre oriented at 45° and 90°. This might have been attributed to the agglomeration of fibres at high fibre content.

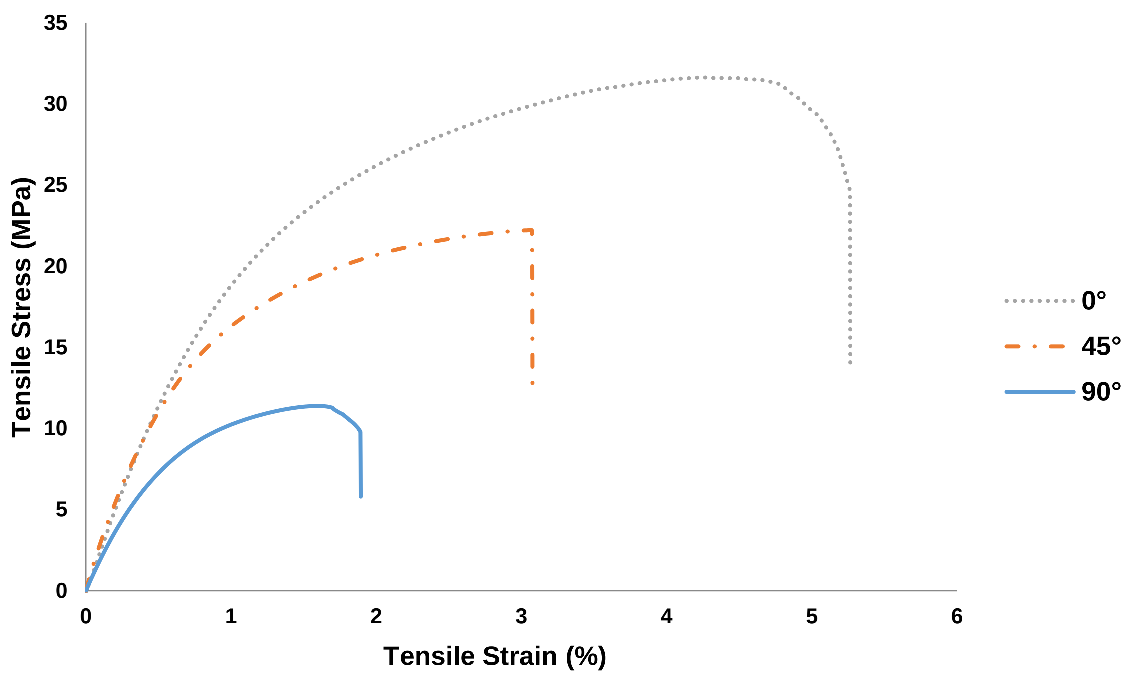

Fig. 4. Tensile stress-strain curves of 25 wt% OPEFB fibre/PP composite

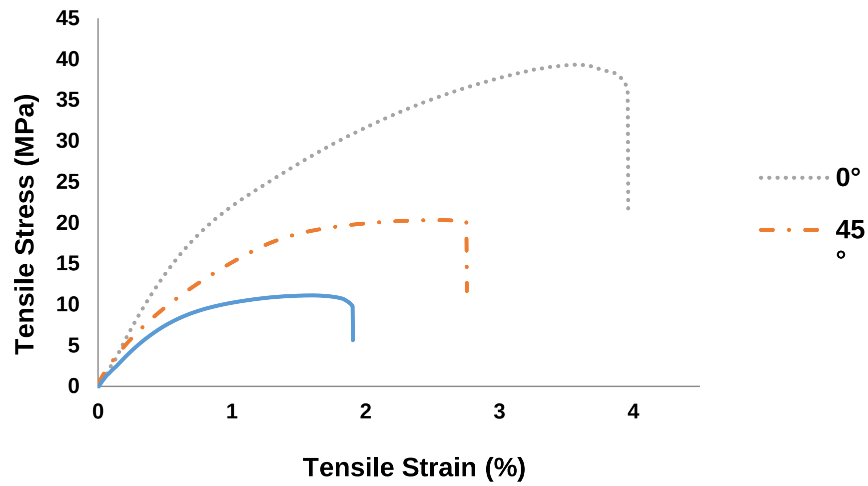

Fig. 5. Tensile stress-strain curves of 35 wt% OPEFB fibre/PP composite

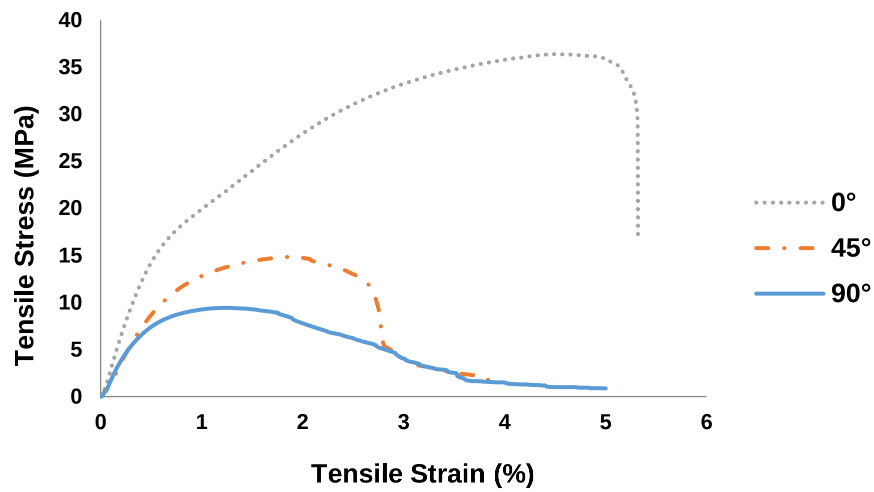

Fig. 6. Tensile stress-strain curves of 45 wt% OPEFB fibre/PP composite

Figure 7 shows the comparison of the tensile strength for the OPEFB fibre/PP composites with various fibre orientation angles and weight ratios. The tensile strengths of the composites decreased with increasing fibre reinforcement angle. This result indicates that the composite can sustain higher tensile load when the reinforcement fibre was aligned parallel with the direction of the applied load. The highest tensile strength of 38.7 MPa obtained for the OPEFB fibre/PP composite was found at the 0° fibre reinforcement angle with 35 wt% fibre ratio. This was approximately 130% greater than the tensile strength of pure PP. When the load was applied parallel with the direction of fibre, the fibre was strained by the same amount as the matrix. Hence, deformation was expected to be uniform for both the fibre and the matrix. This in turn will cause the stiffer fibre to carry a higher amount of stress. Contrarily, when the load applied was not in the fibre direction, the fibre acted like a hard inclusion in the matrix and prevented the distribution of stresses throughout the matrix, which in turn caused higher concentration of localized stresses (Manikandan Nair *et al*. 1996).

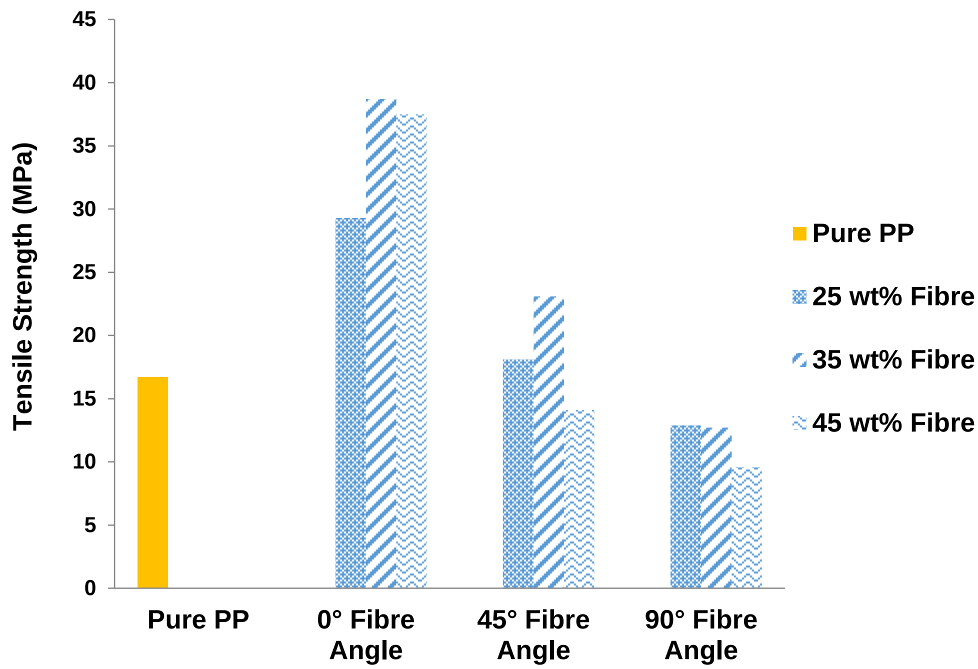

Fig. 7. Tensile strength of the unidirectional OPEFB fibre/PP composites with various fibre loadings and orientation angles

As shown in Fig. 7, when the fibre ratio increased from 25 wt% fibre to 35 wt% fibre, the tensile strength of the composite also increased for each fibre orientation angle except for the fibre with 90° fibre angle. Further increases of fibre ratio to 45 wt% resulted in a decline of tensile strength for the composite. For 0° fibre orientation angle, there was an increase of approximately 32% in tensile strength when the fibre ratio was increased from 25% to 35%. The tensile strength changed from 29.3 MPa to 38.7 MPa for 25% and 35% fibre loadings, respectively. The further increase in fibre ratio to 45% resulted in a decrease of the tensile strength to 37.5 MPa. This was mainly attributed to the wettability of PP in the fabrication process. Figure 8 shows that, at a fibre ratio of 45 wt%, certain parts of the PP matrix, which was placed in the middle during the fabrication process, could not melt and were consequently unable to impregnate the fibre. Therefore, the impregnation of fibres was only dependent on the PP sheets placed at the outer layers during fabrication. Reduced matrix impregnation thereby restricted the matrix from having full access to the fibre surface, which consequently led to an inefficient stress transfer when subjected to tensile load. This explains the reduction of the tensile strength when the fibre ratio was increased from 35 wt% to 45 wt%. The agglomeration of fibre at high fibre content prevented the matrix from melting during the manufacturing process and resulted in poor strength. Similar findings were also observed by Bledzki and Gassan (1999), Pfister and Larock (2010), and Malaba and Jiajun (2015). Poor dispersion due to the high proximity of fibres to one another led to the presence of the weak, unreinforced matrix-only areas. Another factor that may have led to the decrease of tensile strength at high fibre content was the fibre alignment. As the quantity of fibre increased, the technique of manually aligning the fibres for the composite preparation became less reliable, as the tendency of the fibres to be misaligned also increased. The misaligned fibres hence did not contribute effectively to carrying the stress when load was applied.

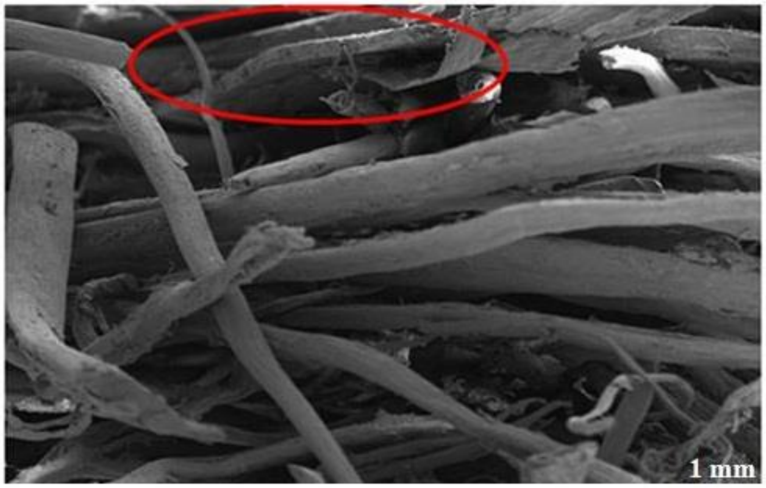

Fig. 8. PP matrix unable to impregnate fibres at 45 wt% OPEFB/PP composite

An electron micrograph of the damage region in the fractured tensile specimens is shown in Fig. 9. As shown, the damage mechanism for the tensile specimens with 0° fibre orientation contributed substantially to fibre fracture with minimum fibre shearing. In contrast, the fibre damage for the 90° oriented fibre was dominated by fibre matrix debonding and matrix cracking, as shown in Fig. 10.

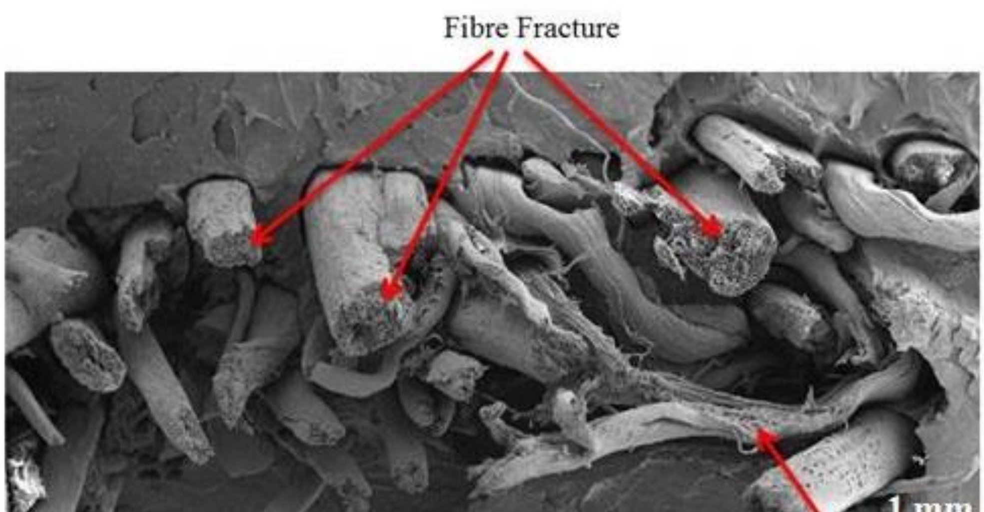

Fig. 9. Electron micrograph of the 0° 35 wt% OPEFB/PP composite tensile specimen fractured surface

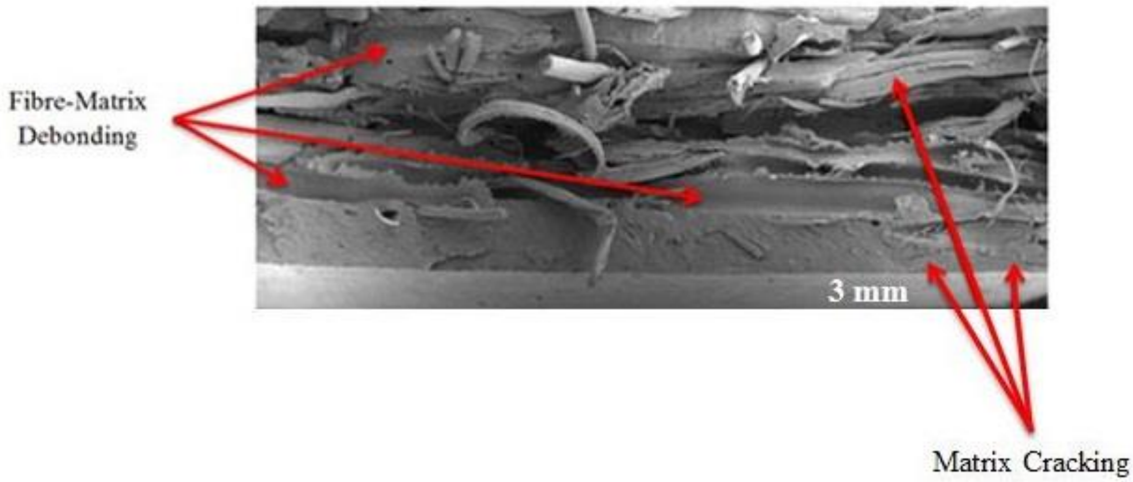

Fig. 10. Electron micrograph of the 90° 35 wt% OPEFB/PP composite tensile specimen fractured surface

Figures 11, 12, and 13 show the load displacement curves for the OPEFB fibre/PP composites with 25 wt%, 35 wt%, and 45 wt% fibre ratios, respectively, under flexural load. For all fibre orientations and fibre ratios, the load displacement curves were characterized by an initially linear region up to a displacement of approximately 2 mm, then nonlinearity until peak load, followed by gradual softening.

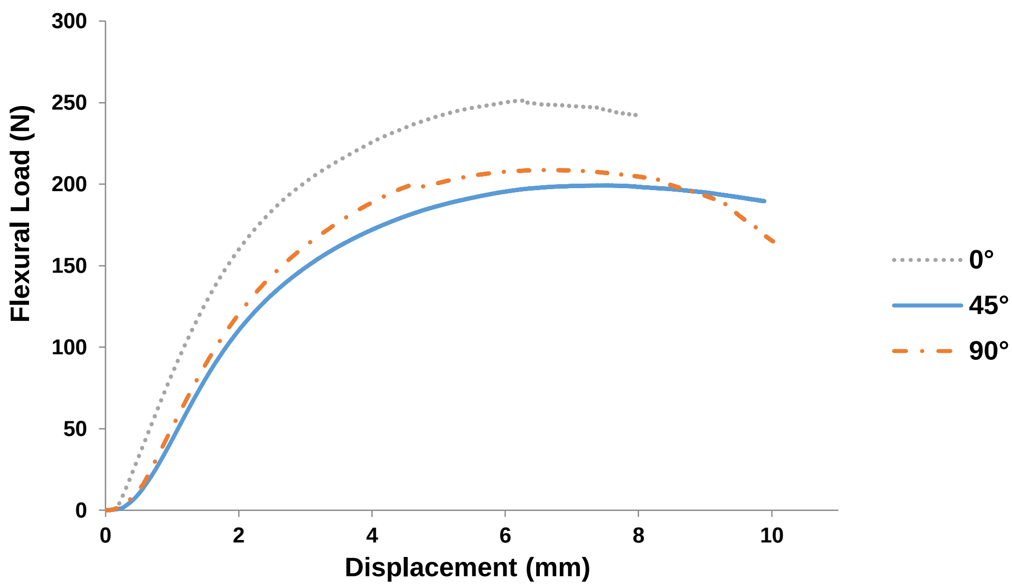

Fig. 11. Load-displacement curves of 25 wt% OPEFB fibre/PP composite under flexural load

For all fibre ratios, the composite with 0° fibre orientation sustained a higher load with higher displacement, as compared to the composites with fibre oriented at 45° and 90° angles. Comparing the three figures, it was apparent that the total displacement to peak load increased with increasing fibre ratio. For the 0° fibre oriented composite, the displacement to peak load showed an increase of approximately 33% from 6.3 mm to 8.4 mm when the fibre ratio increased from 25 wt% to 35 wt%. Further increase of fibre ratio to 45 wt% resulted in an increment of approximately 5% from 8.4 mm to 8.9 mm displacement at peak load. Although the displacement to peak load increased when the fibre ratio increased from 25 wt% to 35 wt%, the peak load decreased approximately 10% from 251 N to 226 N. The peak load increased to 278 N when the fibre ratio was increased to 45 wt%.

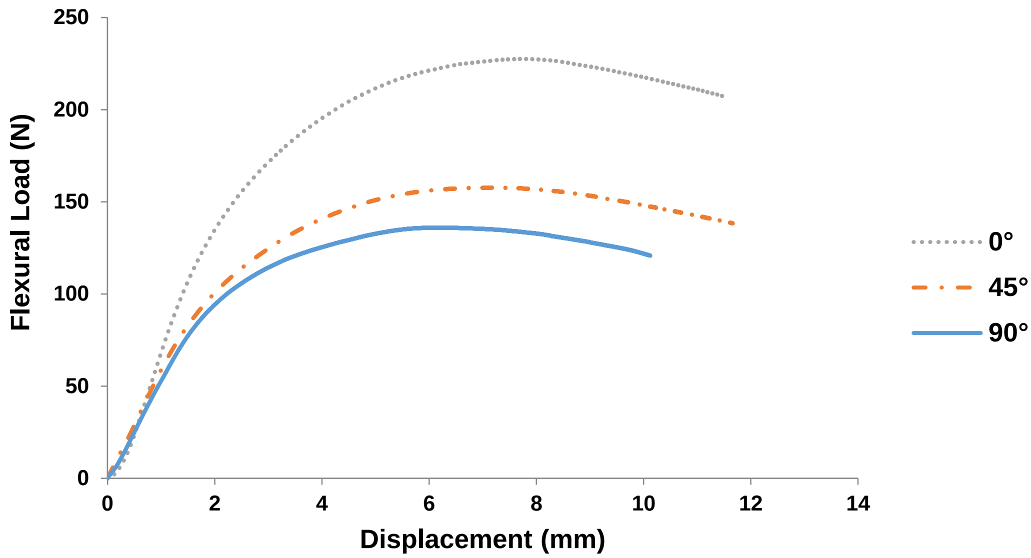

Fig. 12. Load-displacement curves of 35 wt% OPEFB fibre/PP composite under flexural load

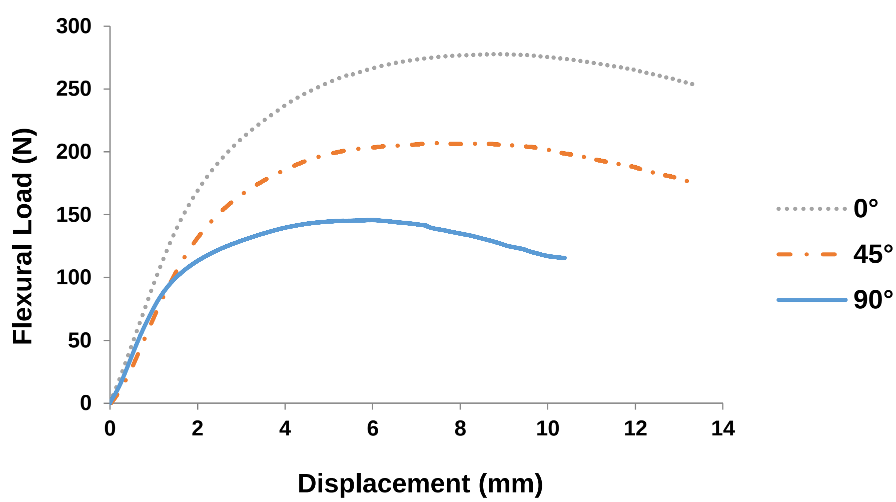

Fig. 13. Load-displacement curves of 45 wt% OPEFB fibre/PP composite under flexural load

The flexural strength of the OPEFB fibre/PP composite is shown in Fig. 14. Similar to tensile strength, an increase in the fibre reinforcement angle resulted in a reduction in the flexural strength of the composite. The 25 wt% OPEFB fibre/PP composite with 0° fibre reinforcement angle exhibited the greatest flexural strength of 145 MPa, greater by approximately 328% when compared with the flexural strength of pure PP. Increasing the fibre loading from 25 wt% to 35 wt% reduced the flexural strength of the composite. Further addition of the fibre to 45 wt% yielded an improvement in the flexural strength.

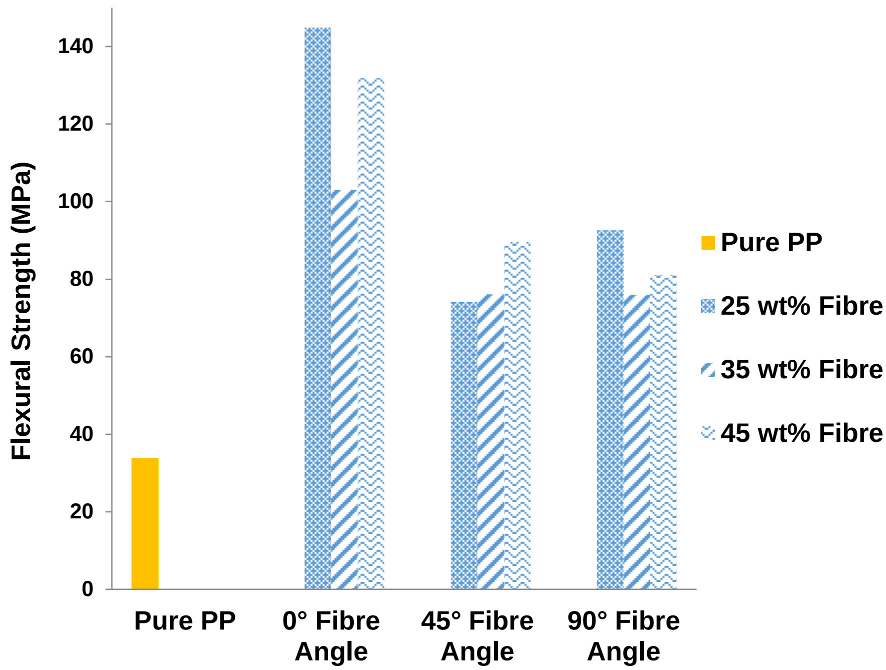

Fig. 14. Flexural strength of OPEFB fibre/PP composite with various fibre loadings and orientation angles

Figure 15 shows the flexural modulus of the OPEFB fibre/PP composite with respect to the fibre orientation angle and fibre ratio.

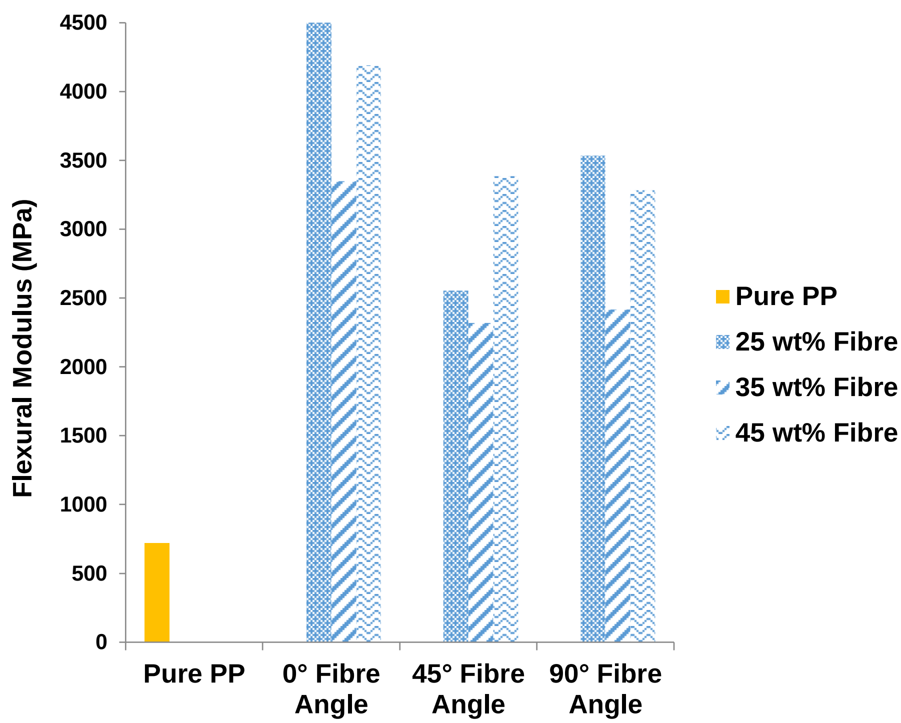

Fig. 15. Flexural modulus of OPEFB/PP composite with various fibre loadings and orientation angles

Incorporation of the OPEFB fibre increased the flexural modulus of PP by approximately 525%. The poor flexural modulus of PP was compensated by the OPEFB fibre. The composite possessed a greater flexural modulus when the fibre was oriented at a 0° angle, as compared with the 45° and 90° orientation angles. It was observed that that the failure for the 90° oriented composite under flexural load was governed mainly by matrix cracking, which propagated through the width and thickness of the specimen. This result was in agreement with Turla *et al*. (2014). The study reported that, under flexural load, cracking propagated across the length of the specimen, with fibre breakage occurring perpendicular to the crack propagation. In this orientation, fibres was parallel with the direction of crack propagation. The orientation thereby requires the matrix to be the main load-carrying member. In contrast, the 0° fibre angle composite acted as a barrier preventing crack propagation. A photograph of the failed specimens is shown in Fig. 16. The specimen at the top represents the OPEFB fibre/PP composite with a 90° fibre orientation, which exhibited cracking that propagated across the width and through the thickness until near to the top part of the specimen.

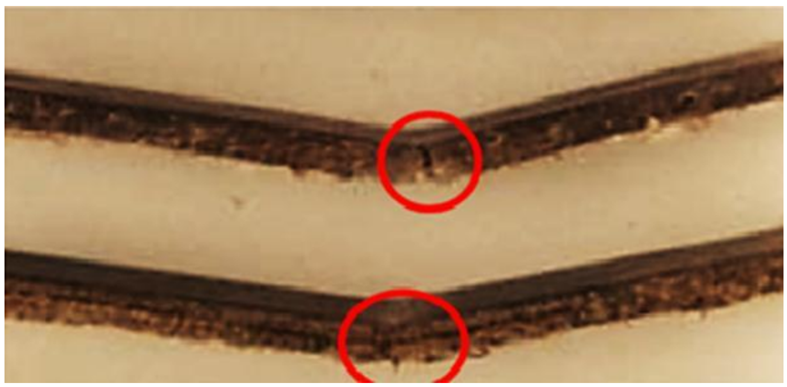

Fig. 16. Photograph of failed specimens of OPEFB fibre/PP composites under flexural load

Although poor wettability was observed for the 45 wt% OPEFB fibre/PP composite, the modulus and flexural strength were greater than the composite with the 35 wt% fibre ratio. The increased rigidity of the 45 wt% OPEFB fibre/PP composite was mainly attributed to the increase in composite thickness due to fibre agglomeration and the thickness of the unmelted PP sheet. Figure 17 shows a comparison of thicknesses for the 35 wt% and 45 wt% composites.

Fig. 17. Failed specimens of 35 wt% and 45 wt% OPEFB fibre/PP composite

Figure 18 shows the impact strengths of the OPEFB fibre/PP composites. The impact strength for the pure PP was 3.32 J. Reinforcement of PP with 45 wt% OPEFB fibre oriented at a 0° angle resulted in an increase of the impact strength to 5.06 J. For all fibre ratios, the composites with the fibre oriented at 45° and 90° angles exhibited lower impact strengths, as compared to those with the fibre oriented at a 0° angle. However, the impact strengths remained greater than that of pure PP. The increase of impact strength with fibre reinforcement indicated that the fibre was capable of acting as the energy-absorbing mechanism during impact.

Increasing the fibre ratio led to an increase in the impact strength, which suggested that the agglomeration of the fibre at a high fibre ratio increased the amount of energy absorbed during impact.

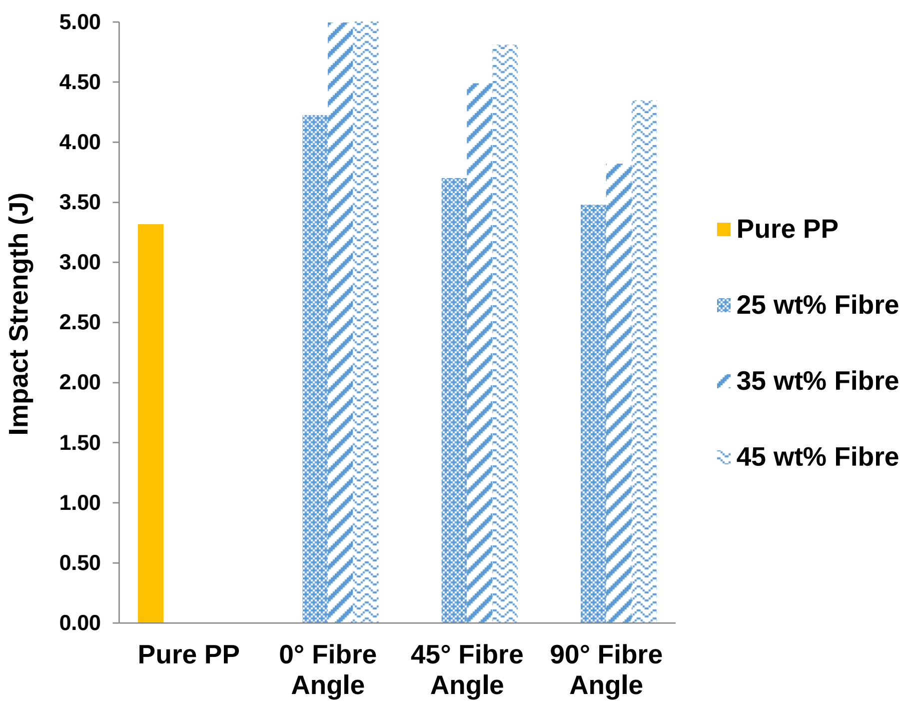

Fig. 18. Impact strength of OPEFB fibre/PP composite with various fibre loadings and orientation angles

Crash Performance of OPEFB Fibre/PP Composite Car Bumper Fascia Using Finite Element Analysis

The aim of adapting the biocomposite material for use in car bumper applications was to maximize the energy absorption by the material in the event of a collision. This consequently reduces the impact experienced by passengers and the risk of fatal injuries. The crash performance was analysed based on the material's energy absorption and peak force upon impact. The crash performance of the composite material was compared with the performance of PP, the conventional material currently employed in car bumper fascias.

Figures 19 and 20 show the energy history plots of PP and OPEFB fibre/PP composite bumper fascias under low-velocity impact, respectively. As shown, the impact terminated at approximately 0.335 s for both materials.

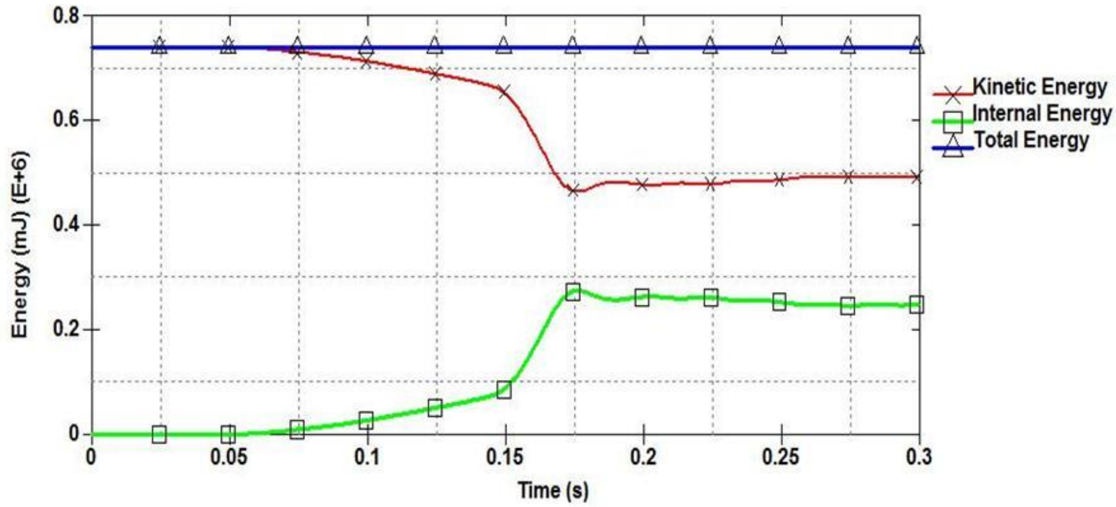

Fig. 19. Energy history plot for impact of PP bumper fascia

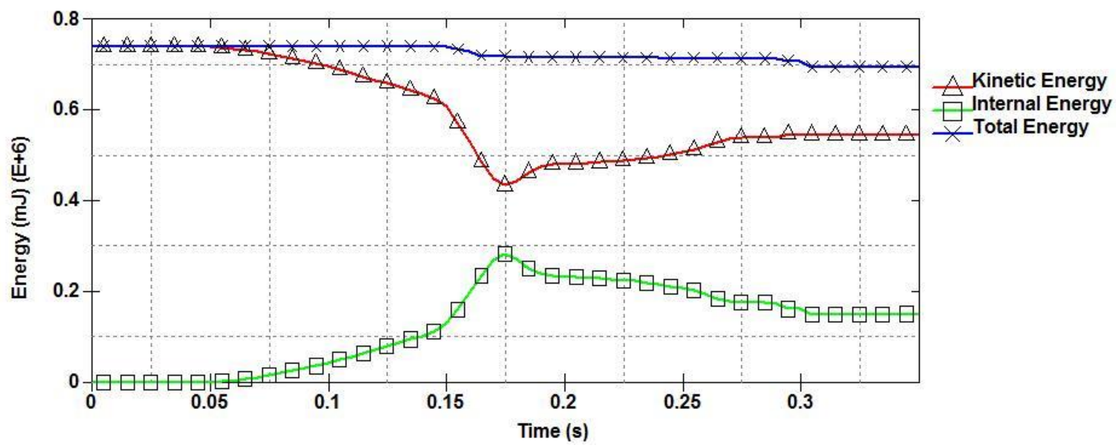

Fig. 20. Energy history plot for impact of OPEFB fibre/PP composite bumper fascia

Figure 21 compares the energy history plots of the PP and the OPEFB fibre/PP composite. The energy absorption capability was measurable through the difference of peak internal energy and terminal internal energy (Hu *et al*. 2015). The composite bumper fascia showed a terminal internal energy of 209 J, which was approximately 16% lower than that of the PP bumper fascia. This result reflected that the energy absorption capability of the composite bumper fascia was greater than that of the PP bumper fascia. The energy absorption capability was improved 219% with the incorporation of the OPEFB fibre, as summarized in Table 2.

The utilization of this OPEFB fibre/PP car bumper fascia hence serves not only for aesthetics but also as one of the structural components. The specific energy absorption (SEA) for both materials is shown in Table 3. Specific energy absorption is a measure of the energy absorption efficiency. Higher values of SEA indicate greater efficiency. The SEA is expressed mathematically as the ratio of the maximum internal energy absorption to the mass of the bumper. The SEA of the composite bumper fascia was approximately 8% greater than that of the PP bumper fascia.

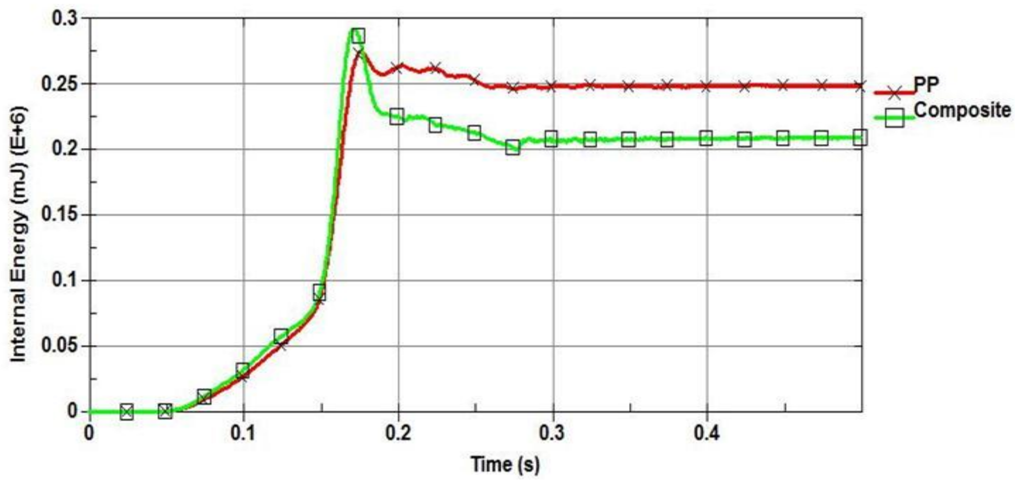

Fig. 21. Comparison of the internal energy–time characteristics of PP and composite bumper fascias

Table 2. Energy Absorption Capabilities for Bumper Fascias of Different Materials

Material	Peak Energy (J)	Terminal Energy (J)	Energy Absorption (J)
PP	275	249	26
Composite	292	209	83

Table 3. Specific Energy Absorption Capabilities of Bumper Fascias

Material	Mass (kg)	Maximum Internal Energy Absorption (J)	Specific Energy Absorption (J/kg)
PP	3.01	275	91.36
Composite	2.95	292	98.98

A comparison of force history plots for the rigid wall after being subjected to low-velocity impact with PP and composite bumper fascias is shown in Fig. 22. Due to the higher stiffness of the composite as compared to PP, the force required to initiate damage in the composite bumper fascia was greater. The peak force experienced by the composite bumper fascia was 27.1 kN, which occurred at approximately 0.169 s, while the peak force for the PP bumper fascia occurred at approximately 0.173 s with a value of 20.1 kN. These peak forces led to maximum deformation to the bumper fascia. The deformation contour maps for the PP and composite bumper fascias are shown in Figs. 23 and 24, respectively. The maximum deformation was approximately 213.6 mm for the PP bumper fascia and 221 mm for the composite bumper fascia. The deformation patterns for both materials were nearly identical.

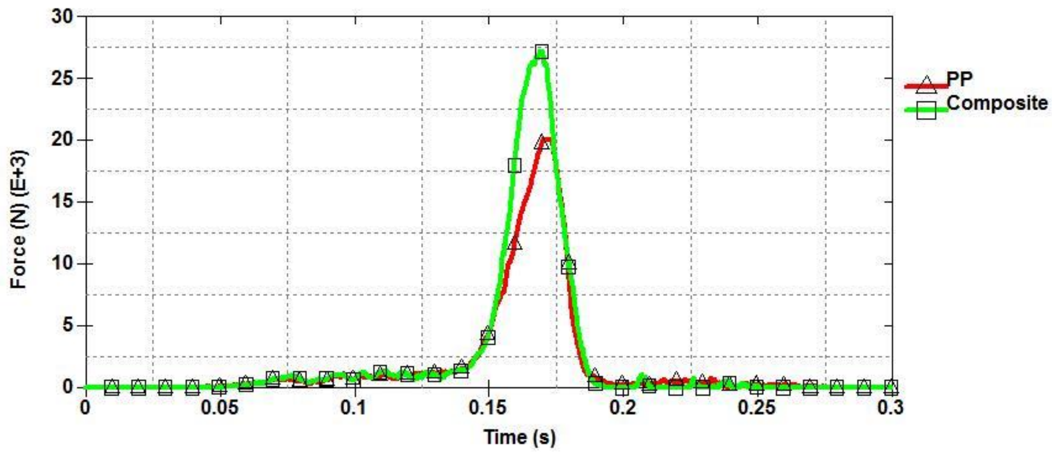

Fig. 22. Comparison of the force–time characteristics of PP and composite bumper fascia impacts

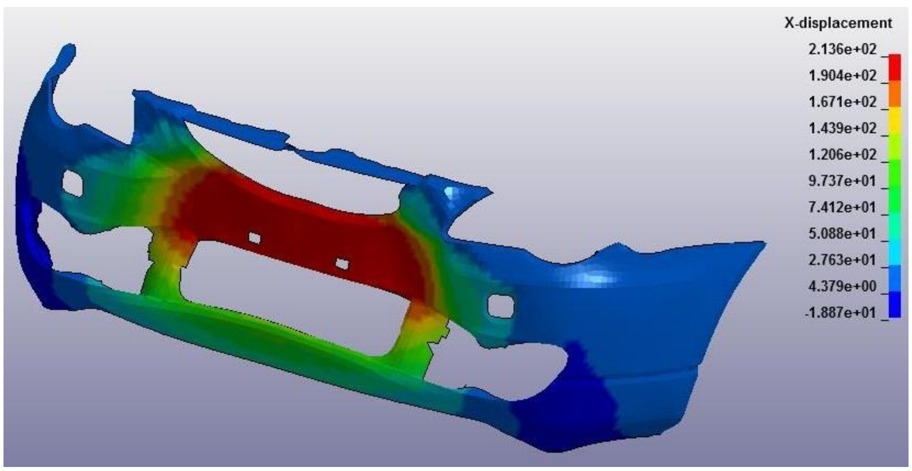

Fig. 23. Deformation of PP bumper fascia under low-velocity frontal impact

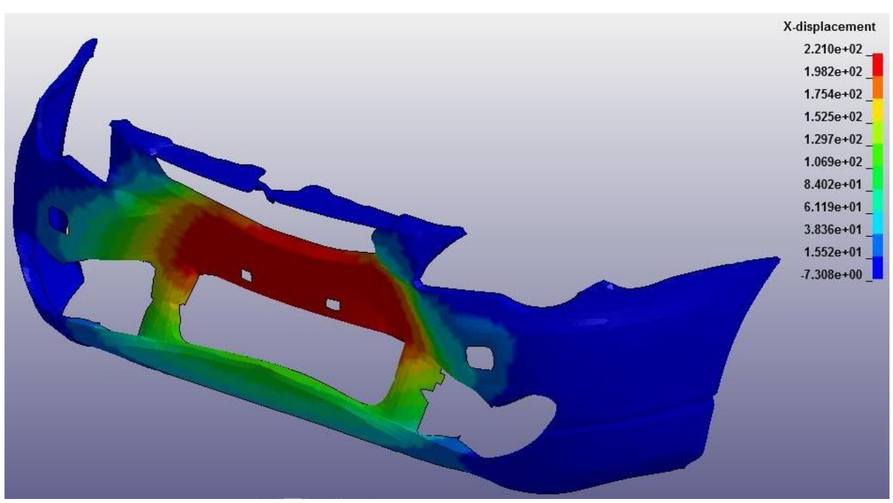

Fig. 24. Deformation of OPEFB fibre/PP composite bumper fascia under low-velocity frontal impact

CONCLUSIONS

The mechanical properties of unidirectional OPEFB fibre/PP composites were studied using tensile, flexural, and impact experimental techniques. The effects of fibre orientation angles and fibre weight ratios were investigated.

1. The tensile stress-strain curves exhibited linear elastic deformation followed by plastic deformation before peak stress for all fibre orientation angles and fibre weight ratios. Abrupt failure was observed after the peak stress except for 45 wt% OPEFB fibre/PP composites with 45° and 90° fibre orientation angles, which showed a highly ductile response until failure. The flexural load-displacement curves revealed the elasto-plastic behaviour of the composites followed by a gradual softening after peak load. The displacement to peak load increased with increasing fibre weight ratios. The tensile, flexural, and impact properties were dependent upon the fibre orientation angles, and composites with 0° fibre orientation exhibited the highest strength values for each property studied. Improvements of approximately 131%, 328%, and 52% in the tensile, flexural, and impact strengths, respectively, were seen in the unidirectional OPEFB fibre/PP composite as compared to the pure PP.
2. Finite element analysis was conducted to compare the crash performances of the unidirectional OPEFB fibre/PP composite bumper fascia with the conventional PP bumper fascia under low-velocity impact. The OPEFB fibre/PP composite bumper fascia showed an ability to offer higher energy absorption capability, of approximately 219% compared to the PP bumper fascia. The specific energy absorption of the composite bumper fascia was comparable to that of the PP bumper fascia.

ACKNOWLEDGMENTS

The authors would like to thank the Department of Mechanical and Manufacturing Engineering, Universiti Putra Malaysia (UPM), Serdang, Malaysia and the Institute of Tropical Forestry and Forest Products (INTROP), UPM, Serdang, Malaysia for their assistance in this research project.

REFERENCES CITED

Abdullah, N., and Sulaiman, F. (2013). “The oil palm wastes in Malaysia,” in: *Biomass Now – Sustainable Growth and Use*, IntechOpen, London, UK.

Aldousiri, B., Alajmi, M., and Shalwan, A. (2013). “Mechanical properties of palm fibre reinforced recycled HDPE,” *Advances in Materials Science and Engineering* 2013, Article ID 508179, 1-7. DOI: 10.1155/2013/508179

Biswas, S., Shahinur, S., Hasan, M., and Ahsan, Q. (2015). “Physical, mechanical and thermal properties of jute and bamboo fiber reinforced unidirectional epoxy composites,” *Procedia Engineering* 105, 933-939. DOI: 10.1016/j.proeng.2015.05.118

Bledzki, A. K., and Gassan, J. (1999). “Composites reinforced with cellulose based fibers,” *Progress in Polymer Science* 24(2), 221-274. DOI: 10.1016/S0079-6700(98)00018-5

Campbell, F. (2003). *Manufacturing Processes for Advanced Composites*, Elsevier, Oxford, UK.

Davoodi, M. M., Sapuan, S. M., Aidy, A., Abu Osman, N. A., Oshkour, A. A., and Wan Abas, W. A. B. (2012). "Development process of new bumper beam for passenger car: A review," *Materials & Design* 40, 304-313. DOI: 10.1016/j.matdes.2012.03.060

Davoodi, M. M., Sapuan, S. M., and Yunus, R. (2008). "Conceptual design of a polymer composite automotive bumper energy absorber," *Materials & Design* 29(7), 1447-1452. DOI: 10.1016/j.matdes.2007.07.011

Hegde, A., Darshan, R. S., Mulla, F., Shoeb, M., and Rajanish, M. (2015). "Tensile properties of unidirectional glass/epoxy composites at different orientations of fibres," *International Journal of Engineering Research and Appl.* 5(3), 150-153.

Hu, Y., Liu, C., Zhang, J., Ding, G., and Wu, Q. (2015). "Research on carbon fiber–reinforced plastic bumper beam subjected to low-velocity frontal impact," *Advances in Mechanical Engineering* 7(6), 1-15. DOI: 10.1177/1687814015589458

Lee, S., Shi, S. Q., Groom, L. H., and Xue, Y. (2010). "Properties of unidirectional kenaf fiber–polyolefin laminates," *Polymer Composites* 31(6), 1067-1074. DOI: 10.1002/pc.20893

Malaba, T., and Jiajun, W. (2015). "Unidirectional cordenka fibre-reinforced furan resin full biocomposite: Properties and influence of high fibre mass fraction," *Journal of Composites* 2015, Article ID 707151, 1-8. DOI: 10.1155/2015/707151

Malkapuram, R., Kumar, V., and Negi, Y. S. (2008). "Recent development in natural fiber reinforced polypropylene composites," *Journal of Reinforced Plastics and Composites* 28(10), 1169-1189. DOI: 10.1177/0731684407087759

Manikandan Nair, K. C., Diwan, S. M., and Thomas, S. (1996). "Tensile properties of short sisal fiber reinforced polystyrene composites," *Journal of Applied Polymer Science* 60(9), 1483-1497. DOI: 10.1002/(SICI)1097-4628(19960531)60:9<1483::AID-APP23>3.0.CO;2-1

Pfister, D. P., and Larock, R. C. (2010). "Green composites from a conjugated linseed oil-based resin and wheat straw," *Composites Part A: Applied Science and Manufacturing* 41(9), 1279-1288. DOI: 10.1016/j.compositesa.2010.05.012

Sapiai, N., Jumahat, A., and Hakim, R. N. (2014). "Tensile and compressive properties of hybrid carbon fiber/ kenaf polymer composite," *Advances in Environmental Biology* 8(8), 2655-2661.

Sapuan, S. M., Maleque, M. A., Hameedullah, M., Suddin, M. N., and Ismail, N. (2005). "A note on the conceptual design of polymeric composite automotive bumper system," *Journal of Materials Processing Technology* 159(2), 145-151. DOI: 10.1016/j.jmatprotec.2004.01.063

Tanwer, A. K. (2014). "Mechanical properties testing of uni-directional and bi-directional glass fibre reinforced epoxy based composites," *International Journal of Research in Advent Technology* 2(11), 34-39.

Turla, P., Kumar, S. S., Reddy, P. H., and Shekar, K. C. (2014). "Processing and flexural strength of carbon fiber and glass fiber reinforced epoxy-matrix hybrid composite," *International Journal of Engineering Research & Technology* 3(4), 394-398.

Article submitted: June 16, 2018; Peer review completed: Sept. 9, 2018; Revised version received: Sept. 13, 2018; Accepted: Sept. 17, 2018; Published: September 20, 2018.
DOI: 10.15376/biores.13.4.8310-8328